



A boundary layer analysis for determination of the limiting current density in an electrodialysis desalination

Akira Nakayama^{a,b,*}, Yoshihiko Sano^a, Xiaohui Bai^a, Kenji Tado^a

^a Dept. of Mechanical Engineering, Shizuoka University, 3-5-1 Johoku, Naka-ku, Hamamatsu 432-8561, Japan

^b School of Civil Engineering and Architecture, Wuhan Polytechnic University, Wuhan, Hubei 430023, China

HIGHLIGHTS

- A novel boundary layer analysis is proposed for an electrodialysis desalination.
- Asymptotic similarity solutions were obtained for electrodialysers with and without spacers.
- A volume average theory was introduced for analyzing electrodialysers with spacers.
- The present analysis agrees well with the experimental data of limiting current density.
- The model can be used to design practical electrodialysers with spacers.

ARTICLE INFO

Article history:

Received 27 August 2016

Received in revised form 9 October 2016

Accepted 25 October 2016

Available online 3 November 2016

Keywords:

Limiting current density

Electrolysis

Ion transport

Desalination

ABSTRACT

A general ion-transport equation has been derived eliminating the electrophoresis term from the set of Nernst-Planck equations for cations and anions, under the local electro-neutrality assumption. Boundary layer solutions were obtained for the two asymptotic cases of sufficiently short and long channels, respectively, when the electric current is applied uniformly across the channels. A local volume averaging theory for porous media was also introduced to describe the cases of electrodialysis stacks with spacers. The results obtained for both with and without spacers are compared against available experimental data. The predicted limiting current density and stack voltage based on the asymptotic solutions for sufficiently short channels agree well with those of measurements for both cases with and without spacers, revealing the validity of the present analysis based on the local electro-neutrality assumption. It has been clearly shown that the spacers work to delay possible depletion of the ions on the dilute side of the membrane, thus increasing the limiting current density.

© 2016 Elsevier B.V. All rights reserved.

1. Introduction

Electrodialysis, which exploits an electrochemical separation process, is a quite effective means to treat brackish water, since it is versatile with respect to avoiding possible scaling and fouling. It has been a common practice to use an electrodialyser for water desalination, so as to remove dissolved minerals such as salts from seawater, wastewater or brackish water e.g. [1,2,3,4]. The electrodialysis process has advantages over conventional distillation techniques and other membrane based processes such as those using reverse osmosis [5], since, in this electrodialysis process, small quantity of dissolved species are removed away from large quantity of feed water rather than removing the large quantity of water from the small quantity of feed water, as in reverse osmosis.

The electrodialyser uses ion-exchange membranes e.g. [1] to transfer ions from dilute to concentrate chambers under the influence of an applied electric potential difference. The ion-exchange membrane electrodialysis stack, as shown in Fig. 1, consists of two electrodes, namely, anode and cathode. Between these electrodes, a number of dilute and concentrate channels are positioned to transfer ions through the ion-exchange membranes.

A unit cell in the stack refers to as a pair of adjacent dilute and concentrate channels formed by an anion exchange membrane (A. E. M.) and a cation exchange membrane (C. E. M.). These two kinds of membranes are placed alternately under the applied electric field. As the ions transfer through the membranes, the dilute cell loses the ions while the adjacent concentrate cell collects them. Thus, the bulk ion concentration in the dilute cell decreases while the that in the concentrate cell increases as the feed water, supplied from below, flows upward to the exit.

A substantial number of researchers attacked the Nernst-Planck equation, to investigate the ion transport from the dilute channel to

* Corresponding author at: Dept. of Mechanical Engineering, Shizuoka University, 3-5-1 Johoku, Hamamatsu 432-8561, Japan.

E-mail address: nakayama.akira@shizuoka.ac.jp (A. Nakayama).

Nomenclature

c	ion concentration [mol/m ³]
D_i	diffusion coefficients of cation ($i = 1$) and anion ($i = 2$) [m ² /s]
D_e	effective diffusion coefficient $D_e = (1 - \frac{z_1}{z_2}) / (\frac{1}{D_1} - \frac{z_1}{z_2} \frac{1}{D_2})$ [m ² /s]
F	Faraday constant [96,485C/mol]
i_j	current density vector, $i_j = (0, i, 0)$ [A/m ²]
i_{lim}	limiting current density [A/m ²]
L	channel length [m]
n	coordinate outward normal to the membrane surface $n + y = W/2$
R	gas constant [8,314 J/mol K]
T	temperature [K]
u_j	velocity vector [m/s]
u	velocity component in x direction [m/s]
v	velocity component in y direction [m/s]
W	channel width [m]
x	vertical coordinate [m]
y	transverse coordinate measured from the axis of symmetry [m]
z	valency of an ion [–]
Greek symbols	
δ	concentration boundary thickness [m]
ε	porosity [–]
ς	ratio of the concentrate compartment width to the dilute channel width compartment [–]
η	similarity variable [–]
ν	kinematic viscosity [m ² /s]
ξ	empirical coefficient for mechanical dispersion [–]
ρ	density [kg/m ³]
φ	voltage [V]
Subscript	
c	concentrate
d	dilute
e	effective
dis	dispersion
m	membrane
Others	
$\langle \phi \rangle$	Darcian average
$\langle \phi \rangle^f$	intrinsic volume average
$\bar{\phi}$	Bulk mean

concentrate channel through membranes e.g. [6,7,8]. Most of these investigations focus on one-directional ion transport across the channels and membranes. However, it is the role of thin concentration boundary

layer that determines the electrolysers performance. Therefore, we must take full account of the boundary layer nature hidden in the Nernst-Planck equation.

In the dilute channel boundary layer, the ionic concentration decreases towards the C. E. M., whereas, in the concentrate channel, the ionic concentration, which is higher than that of the dilute channel, decreases away from the C. E. M., which is called “concentration polarization”. A thinner boundary layer allows a steeper concentration at the membrane surfaces, thus, allowing a greater electric current to pass through the membrane. The electric current density that causes zero concentration on the ion exchange membranes as the result of excessive concentration polarization is termed as “limiting current density” e.g. [9, 10]. This limiting current density is of great importance in practical applications, since, just under this limiting current density, the maximum ionic separation rate can be achieved in the electrolysers without violating the electro-neutrality. When the limiting current density is exceeded, the electrical resistance in the dilute solution increases drastically due to the depletion of the ions within the boundary layer. The current above the limiting value is called “overlimiting current”. Thus, any electrolysers operations should be conducted below this limiting current to avoid water dissociation.

There are a number of theoretical and experimental investigations associated with ion concentration boundary layers, including those of Lee et al. [11] and Tanaka [12,13,14]. Tobias et al. [15] provides a review on diffusion and convection of ions in electrolysis and theoretical methods for predicting its diffusion layer. The ion film thickness was estimated for various cases appealing to mass, heat and momentum analogy and dimensional analysis. However, the boundary layer development in a multichannel system in electrolysers has not been treated, perhaps, due to its complexity. Sonin and Probst [16] proposed a hydrodynamic theory of desalination by electrolysers. A classical integral method was used to obtain approximate solutions. An empirical matching formula for the limiting current density was introduced to cover a wide range of operating conditions.

Nevertheless, analytical boundary layer treatments based on the similarity transformations have not been reported in the literature. In this study, a general ion transport equation will be derived from the Nernst-Planck equation under the assumption of local electro-neutrality. The resulting ion transport equation is considered along with the prevailed velocity field. The classical boundary layer treatments established in viscous flows [17] are revisited to obtain possible similarity solutions for the two asymptotic cases of sufficiently short and long channels in the electrolysers, when the electric current is applied uniformly across the channels.

A volume averaging theory will also be introduced for the first time to derive a volume averaged version of the Nernst-Planck equation, which is used to attack the case of electrolysers with spacers [18]. It will be shown that the asymptotic solutions for sufficiently short channels agree well with that of measurement for both cases with and without spacers. This substantiates the validity of the present analysis based on the local electro-neutrality assumption.

2. General ion transport equation

The Nernst-Planck equation in a tensor form describing ion transport of species i in the solution runs as

$$\frac{\partial c_i}{\partial t} + u_j \frac{\partial c_i}{\partial x_j} = \frac{\partial}{\partial x_j} \left(D_i \frac{\partial c_i}{\partial x_j} + \frac{z_i F D_i c_i}{RT} \frac{\partial \varphi}{\partial x_j} \right) \quad (1)$$

where the species is either cation ($i = 1$) or anion ($i = 2$), such as Na⁺ or Cl[–]. The first term on the right hand side of Eq. (1) describes diffusion while the second term describes electrophoresis. D_i is the diffusion coefficient, φ , the voltage, R (= 8,314 J/mol K), gas constant, T , the temperature and F (= 96,485C/mol), Faraday constant. z_i is the species charge

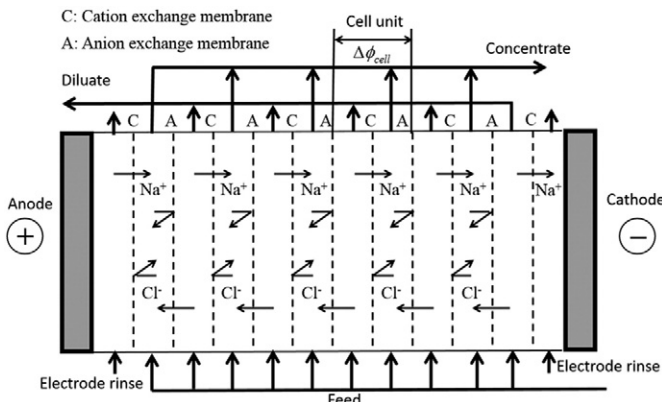


Fig. 1. Electrolysers stack.

number such that $z_1 = 1$ and $z_2 = -1$ for the case of Na^+ and Cl^- and $z_1 = 1$ and $z_2 = -2$ for the case of Na^+ and SO_4^{2-} . Eq. (1) can be written for the cation of z_1 and the anion of z_2 as

$$\frac{\partial c_1}{\partial t} + u_j \frac{\partial c_1}{\partial x_j} = \frac{\partial}{\partial x_j} \left(D_1 \frac{\partial c_1}{\partial x_j} + \frac{z_1 F D_1 c_1}{RT} \frac{\partial \varphi}{\partial x_j} \right) \quad (2a)$$

$$\frac{\partial c_2}{\partial t} + u_j \frac{\partial c_2}{\partial x_j} = \frac{\partial}{\partial x_j} \left(D_2 \frac{\partial c_2}{\partial x_j} + \frac{z_2 F D_2 c_2}{RT} \frac{\partial \varphi}{\partial x_j} \right) \quad (2b)$$

The summation $D_2 \times (2a) + D_1 \times (2b)$ and the division by $(D_2 - (z_1/z_2)D_1)$ yields general ion transport equation:

$$\frac{\partial c_1}{\partial t} + u_j \frac{\partial c_1}{\partial x_j} = \frac{\partial}{\partial x_j} \left(D_e \frac{\partial c_1}{\partial x_j} \right) \quad (3)$$

where

$$D_e = \frac{1 - \frac{z_1}{z_2}}{D_1 - \frac{z_1}{z_2} D_2} \quad (4)$$

is the effective “harmonic” diffusivity. Note that c_2 is eliminated using the local electro-neutrality condition, namely, local electro-neutrality:

$$z_1 c_1 + z_2 c_2 = 0 \quad (5)$$

The electrophoresis term is eliminated from the general ion transport (Eq. (3)) under the local electro-neutrality condition, which enables us to appeal to a classical convection-diffusion boundary layer analysis. Moreover, the summation $z_1 \times (2a) + z_2 \times (2b)$ under the local electro-neutrality condition gives

$$z_1 \frac{\partial}{\partial x_j} \left((D_1 - D_2) \frac{\partial c_1}{\partial x_j} + \frac{F(z_1 D_1 - z_2 D_2)}{RT} c_1 \frac{\partial \varphi}{\partial x_j} \right) = 0$$

where the convection terms vanish under the local electro-neutrality assumption. Note that the diffusion coefficient of the cation D_1 is usually less than that of anion D_2 . The foregoing equation leads to Faraday's law:

$$-z_1 (D_1 - D_2) \frac{\partial c_1}{\partial x_j} - z_1 \frac{F(z_1 D_1 - z_2 D_2)}{RT} c_1 \frac{\partial \varphi}{\partial x_j} = \frac{i_j}{F} \quad (6)$$

where i_j is the current density vector. Once the distribution of the cation concentration c_1 is revealed by solving Eq. (3), the spatial distribution of φ may be obtained for the given current density vector i_j by integrating Eq. (6).

3. Asymptotic solutions for an electrodialyser without spacers

As shown in Fig. 2, a unit cell consisting a pair of dilute and concentrate channels is considered for the analysis. This unit cell can represent any one of cells in the electrodialysis stack, in which the membrane thickness is negligible as compared with the channel width W . The Reynolds number within the channel, namely, $\text{Re} = W \bar{u}_c / \nu$, is usually sufficiently small, so that the flow field throughout the channel is hydro-dynamically fully developed, whereas the ion concentration field in the entrance region is still developing due to comparatively high Schmidt number $\text{Sc} = \nu / D_e$. In what follows, we shall focus on the transport of the sodium chloride ions Na^+ and Cl^- (i.e. $z_1 = 1$ and $z_2 = -1$) within an electrodialyser without spacers.

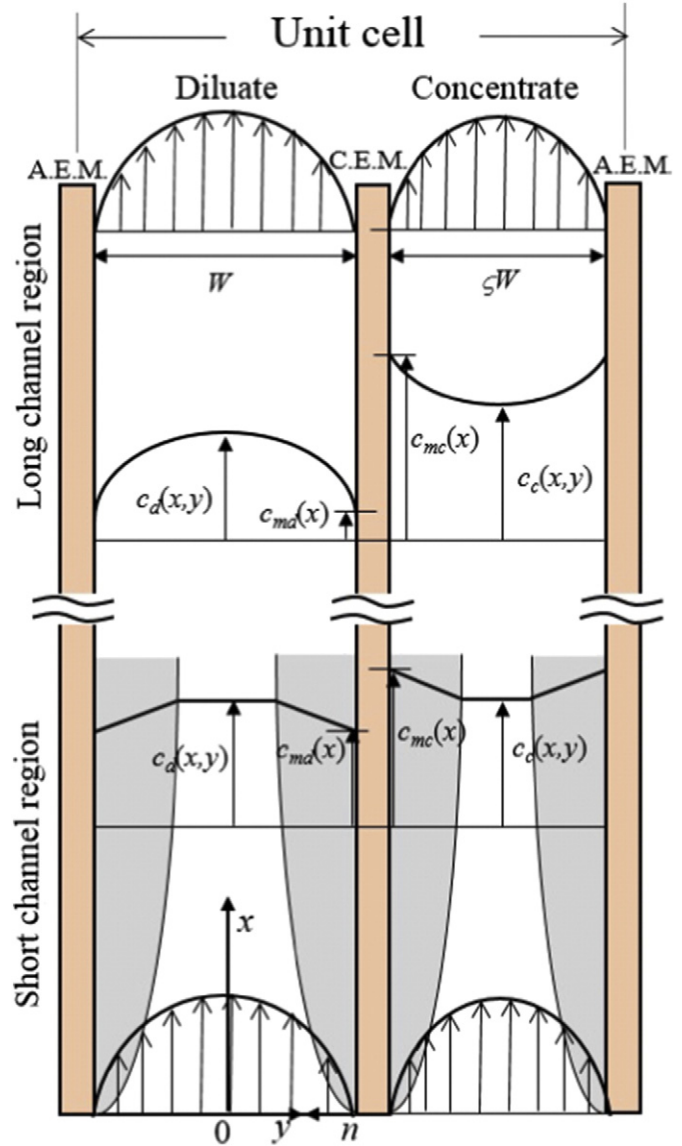


Fig. 2. Unit cell (Short and long channel regions).

3.1. Asymptotic solutions for long channels.

Since the transverse flow across the membrane due to the osmotic pressure is negligible, the following parabolic velocity profile based on the Navier-Stokes equation prevails everywhere in the dilute channel without spacers:

$$u_d(x, y) = \frac{3}{2} \bar{u}_d \left(1 - \left(\frac{y}{W/2} \right)^2 \right) \quad (7a)$$

and

$$v_d(x, y) = 0 \quad (7b)$$

where \bar{u}_d is the bulk mean velocity in the x direction (i.e. feed velocity). The general ion transport (Eq. (3)) can be written for the steady flow in the dilute channel as

$$u_d \frac{\partial c_d}{\partial x} = \frac{\partial}{\partial y} \left(D_e \frac{\partial c_d}{\partial y} \right) \quad (8)$$

where $c_d = c_1 = c_2$ for the case of sodium chloride, while the effective

diffusion coefficient is given according to Eq. (4) by

$$D_e = \frac{2}{\frac{1}{D_1} + \frac{1}{D_2}} \quad (9)$$

Upon noting the concentration boundary layer thickness $\delta(x)$ is of order $\sqrt{D_e x / \bar{u}_d}$ according to the boundary layer (Eq. (8)), we shall first consider the asymptotic case of long channel, namely, $\sqrt{D_e L / \bar{u}_d} \gg W$ (i.e. $\bar{u}_d W^2 / D_e L \ll 1$). As indicated in Fig. 2, we may also define two asymptotic regions, namely, the “long channel” region at $x \gg \bar{u}_d W^2 / D_e$ corresponding to the asymptotic far downstream region in a sufficiently slender channel, and the “short channel” region at $x \ll \bar{u}_d W^2 / D_e$ corresponding to the concentration boundary layer developing region.

Integration of the foregoing Eq. (8) across the dilute channel yields

$$W \bar{u}_d \frac{d\bar{c}_d}{dx} = D_e \frac{\partial c_d}{\partial y} \Big|_{y=W/2} - D_e \frac{\partial c_d}{\partial y} \Big|_{y=-W/2} = -\frac{i}{F}$$

where \bar{c}_d is the bulk mean ion concentration and i is the current density passing through the membrane, which is assumed to be constant. Since the concentration profile is symmetry about $y=0$, we find

$$D_e \frac{\partial c_d}{\partial y} \Big|_{y=W/2} = -D_e \frac{\partial c_d}{\partial y} \Big|_{y=-W/2} = -\frac{i}{2F}$$

Hence, we have

$$W \bar{u}_d \frac{d\bar{c}_d}{dx} = 2D_e \frac{\partial c_d}{\partial y} \Big|_{y=W/2} = -\frac{i}{F} \quad (10)$$

and

$$\frac{d\bar{c}_d}{dx} = \frac{\partial c_d}{\partial x} = -\frac{i}{FW \bar{u}_d} \quad (11)$$

Thus, \bar{c}_d decreases linearly towards the exit:

$$\bar{c}_d(x) = \bar{c}_d(0) - \frac{i}{FW \bar{u}_d} x \quad (12)$$

Eliminating $\partial c_d / \partial x$ from Eq. (8) using Eq. (11), we find

$$-\frac{3}{2} \left(1 - \left(\frac{y}{W/2} \right)^2 \right) \frac{i}{FW} = D_e \frac{d^2(c_d - c_{md})}{dy^2} \quad (13)$$

Exploiting the boundary conditions:

$$c_d|_{y=W/2} = c_{md} \quad (14a)$$

and

$$\frac{d(c_d - c_{md})}{dy} \Big|_{y=0} = 0 \quad (14b)$$

where the concentration on the membrane $c_{md}(x)$ is yet unknown, Eq. (13) can readily be integrated to find the distribution of the concentration across the dilute channel as

$$c_d(x, y) - c_{md}(x) = \frac{Wi}{32FD_e} \left(5 - 6 \left(\frac{y}{W/2} \right)^2 + \left(\frac{y}{W/2} \right)^4 \right) \quad (15)$$

Naturally, the bulk mixed concentration can be found from $\int_0^{W/2} c_d u_d dy / (\bar{u}_d W / 2)$:

$$c_d(x) - c_{md}(x) = \frac{Wi}{32FD_e(\bar{u}_d W / 2)} \int_0^{W/2} \left(5 - 6 \left(\frac{y}{W/2} \right)^2 + \left(\frac{y}{W/2} \right)^4 \right) \frac{3}{2} u_d \left(1 - \left(\frac{y}{W/2} \right)^2 \right) dy = \frac{17}{140} \frac{Wi}{FD_e} \quad (16)$$

From Eqs. (12) and (16), we obtain the concentration on the dilute side of the cation exchange membrane:

$$c_{md}(x) = \bar{c}_d(0) - \frac{17}{140} \frac{Wi}{FD_e} - \frac{i}{FW \bar{u}_d} x \quad (17)$$

The limiting current density i_{lim} is attained when the concentration on the dilute side of the membrane vanishes at the exit, namely, $c_{md}(L) = 0$ such that, for the long channel case, the limiting current density i_{lim} is given by

$$i_{lim} = \frac{\frac{FW \bar{u}_d}{L} \bar{c}_d(0)}{1 + \frac{17}{140} \left(\frac{\bar{u}_d W^2}{D_e L} \right)} = \frac{FW \bar{u}_d}{L} \bar{c}_d(0) \left(1 - \frac{17}{140} \left(\frac{\bar{u}_d W^2}{D_e L} \right) \right) \quad (18)$$

for $\frac{\bar{u}_d W^2}{D_e L} \ll 1$

A similar analysis can be conducted for the concentrate channel of width ζW . In the concentrate channel, the bulk mean concentration $\bar{c}_c(x)$ increases towards the exit as the ions supplied from the dilute channel. As illustrated in Fig. 2, the concentration on the concentrate side of the membrane $\bar{c}_{mc}(x)$ is higher than the bulk mean concentration $\bar{c}_c(x)$. Thus, we have the long channel solutions as follows:

$$\bar{c}_c(x) = \bar{c}_c(0) + \frac{i}{F \zeta W \bar{u}_c} x \quad (19)$$

$$c_c(x, y) - c_{mc}(x) = -\frac{\zeta Wi}{32FD_e} \left(5 - 6 \left(\frac{y}{W/2} \right)^2 + \left(\frac{y}{W/2} \right)^4 \right) \quad (20)$$

$$c_{mc}(x) = \bar{c}_c(0) + \frac{17}{140} \frac{\zeta Wi}{FD_e} + \frac{i}{F \zeta W \bar{u}_c} x \quad (21)$$

3.2. Asymptotic solutions for short channels

We shall now consider the “short channel” region $x \ll \bar{u}_d W^2 / D_e$, in which the concentration boundary layer grows from the inlet as indicated in Fig. 2. Since the boundary layer is so thin, we may approximate the velocity profile across the concentration boundary layer using the first term of the Taylor series expansion as

$$u_d(x, n) = \frac{\partial}{\partial n} \frac{3}{2} \bar{u}_d \left(1 - \left(\frac{y}{W/2} \right)^2 \right) \Big|_{n=0} = 6 \frac{\bar{u}_d}{W} n \quad (22)$$

where the coordinate n is set outward normal to the membrane surface as indicated in Fig. 2 such that

$$y + n = \frac{W}{2} \quad (23)$$

Then, the general ion transport (Eq. (8)) is written for the concentration boundary layer as

$$6 \frac{\bar{u}_d}{W} n \frac{\partial c_d}{\partial x} = \frac{\partial}{\partial n} \left(D_e \frac{\partial c_d}{\partial n} \right) \quad (24)$$

A scale analysis on the foregoing equation reveals that the concentration boundary layer thickness grows as $\delta(x) \sim (D_e W x / \bar{u}_d)^{1/3} \propto x^{1/3}$.

Furthermore, Eq. (10) indicates $(\bar{c}_d(0) - c_{md}(x)) \sim (i / F D_e) \delta(x) \propto x^{1/3}$.

Following the classical boundary layer theory [17], the similarity transformation is introduced as follows:

$$g(\eta) = \frac{c_d(x, n) - \bar{c}_d(0)}{c_{md}(x) - \bar{c}_d(0)} \quad (25)$$

where the similarity variable $\eta \sim n / \delta(x)$ is given by

$$\eta = \frac{n}{x} \left(\frac{\bar{u}_d x^2}{D_e W} \right)^{1/3} \propto \frac{n}{x^{1/3}} \quad (26)$$

Using these similarity variables, Eq. (24) can readily be transformed into the following ordinary differential equation:

$$\frac{d^2 g}{d\eta^2} + 2\eta \left(\eta \frac{dg}{d\eta} - g \right) = 0 \quad (27)$$

which can be integrated with the boundary conditions, namely, $g(0) = 1$ and $g(\infty) = 0$. We may use any standard integration procedure based on the Runge-Kutta-Gill method (e.g. Nakayama [19]) to find

$$\left. \frac{dg}{d\eta} \right|_{\eta=0} = -1.183 \quad (28)$$

Eq. (10) may also be transformed as

$$2D_e \frac{\partial c_d}{\partial y} \Big|_{y=W/2} = -2D_e \frac{c_{md}(x) - \bar{c}_d(0)}{x} \left(\frac{\bar{u}_d x^2}{D_e W} \right)^{1/3} \left. \frac{dg}{d\eta} \right|_{\eta=0} = -\frac{i}{F} \quad (29)$$

Thus, the limiting current density yielding $c_{md}(L) = 0$, is given for the short channel case, by.

$$i_{lim} = 2.366 \frac{F D_e \bar{c}_d(0)}{L} \left(\frac{\bar{u}_d L^2}{D_e W} \right)^{1/3} \text{ for } \frac{\bar{u}_d W^2}{D_e L} \gg 1 \quad (30)$$

Most of the conventional formulas based on the one-dimensional ion transport model run as $i_{lim} \propto F D_1 \bar{c}_d / \delta$ in which \bar{c}_d and δ are the bulk concentration and concentration boundary layer thickness at the location where the concentration vanishes at the dilute side of the membrane. These values are not known a priori, unless the boundary layer development is analyzed solving the set of the 2-dimensional ion transport boundary layer equations, as demonstrated above. Instead of solving the boundary layer equations, these values in the conventional formulas are empirically estimated for given channel height, length, feed concentration and velocity. Such an approach without considering boundary layer effects properly is highly questionable especially when spacers are present within the channels.

4. Asymptotic solutions for an electrodialyser with spacers

Most electrodialysers in industrial applications have spacers between the cation and anion exchange membranes. The spacers are used to hold the adjacent membranes apart to provide a passage for the solutions. Another important role of the spacers is to mix the solutions in the channels, and thus, to delay depletion of ions, increasing

the value of the limiting current density. Flows through channels with spacers may be treated as flows in porous media, in which the volume averaging theory, e.g. [19,20,21,22], may be exploited. In the volume averaging theory, each quantity ϕ is decomposed into its local volume average $\langle \phi \rangle^f$ and spatial derivation $\tilde{\phi}$ from it such that

$$\phi = \langle \phi \rangle^f + \tilde{\phi} \quad (31)$$

With this decomposition, the general ion transport equation may be integrated over a local control volume V , to yield the following volume averaged equation written in terms of the volume averaged quantities:

$$\begin{aligned} \varepsilon \frac{\partial \langle c \rangle^f}{\partial t} + \frac{\partial \langle u_j \rangle^f \langle c \rangle^f}{\partial x_j} \\ = \frac{\partial}{\partial x_j} \left(\varepsilon D_e \frac{\partial \langle c \rangle^f}{\partial x_j} + \frac{D_e}{V} \int_{A_{int}} c n_j dA - \varepsilon \langle \tilde{u}_j \tilde{c} \rangle^f \right) - \frac{1}{V} \int_{A_{int}} u_j c n_j dA \\ + \frac{1}{V} \int_{A_{int}} D_e \frac{\partial c}{\partial x_j} n_j dA \end{aligned}$$

where ε is the porosity (i.e. the volume fraction which the solution occupies), which is usually close to unity. Mathematical details in the volume averaging procedure may be found in a textbook such as [20]. In the equation, the interfacial terms (i.e. the last two RHS terms) vanish due to no-slip and no-ion flux conditions on the interface A_{int} , namely, $u_j = \vec{0}$ and $(\partial c / \partial x_j) n_j = 0$. Furthermore, the tortuosity in ion transport may well be neglected since $\frac{D_e}{V} \int_{A_{int}} c n_j dA \approx \frac{D_e}{V} c \int_{A_{int}} n_j dA = \vec{0}$. Thus, the equations reduce to

$$\varepsilon \frac{\partial \langle c \rangle^f}{\partial t} + \frac{\partial \langle u_j \rangle^f \langle c \rangle^f}{\partial x_j} = \frac{\partial}{\partial x_j} \left(\varepsilon D_e \frac{\partial \langle c \rangle^f}{\partial x_j} - \varepsilon \langle \tilde{u}_j \tilde{c} \rangle^f \right) \quad (32)$$

The second term on the right hand side is the mechanical dispersion term as the result of mechanical mixing due to the presence of porous structure. This mechanical dispersion term may be modeled using the gradient diffusion hypothesis (e.g. [20,23]) as

$$-\varepsilon \langle \tilde{u}_j \tilde{c} \rangle^f = \varepsilon D_{disjk} \frac{\partial \langle c \rangle^f}{\partial x_k} \quad (33)$$

In a passage filled with a porous medium, the Darcy flow (i.e. macroscopically uniform flow) prevails, in which the Darcian velocity vector is given by $\langle u_j \rangle = (\bar{u}_d, 0, 0)$. Note that \bar{u}_d is the apparent bulk mean velocity in a porous channel, namely, the bulk mean velocity of the feed flow at the inlet section without a porous medium. Thus, for the case of the dilute channel with spacers, the equation reduces to

$$\bar{u}_d \frac{\partial \langle c \rangle^f}{\partial x} = \frac{\partial}{\partial y} \left(\varepsilon (D_e + D_{dis}) \frac{\partial \langle c \rangle^f}{\partial y} \right) \quad (34)$$

The effective molecular diffusion part εD_e diminishes for $\varepsilon < 1$. However, its mechanical dispersion counterpart dominates over it, such that $\varepsilon D_{dis} \gg D_e > \varepsilon D_e$.

Zhang et al. [23] in their study in convection in a nanofluid saturated metal foam considered the Taylor dispersion problem, in which the temperature of a thin disk of fluid in the hydro-dynamically fully developed flow is suddenly raised to a certain temperature and the temperature distribution thereafter within the fluid in a tube is sought to find out the thermal dispersion coefficient. They analytically found that the thermal dispersion coefficient is proportional to the product of the mean velocity and some reference length scale (which is consistent with both dimensional analysis and experimental evidence [20]) and subsequently, proposed an analogy between heat and mass transfer analogy. Their analogy can be exploited for the present case of ion

transfer, modeling the transverse dispersion coefficient D_{dis} as

$$D_{dis} = \xi \bar{u}_d W \quad (35)$$

where the coefficient ξ should be determined empirically. Eq. (35) suggests $\xi \bar{u}_d W \sim u_{ref} l_{ref}$ where u_{ref} and l_{ref} are the reference velocity and length scale for additional ion mixing due to the presence of spacers. Thus, ξ roughly gives the ratio $u_{ref} l_{ref} / \bar{u}_d W$, which is naturally expected to be very small, since both \bar{u}_d and W are external macro scales.

4.1. Asymptotic solutions for long channels

Eq. (34) with Eq. (11) can easily be integrated twice to obtain the asymptotic solutions for the long channel regime, as

$$\langle c_d \rangle(x, y) - \langle c_{md} \rangle(x) = \frac{Wi}{8\epsilon D_e \left(1 + \xi \frac{\bar{u}_d W}{D_e}\right)} \left(1 - \left(\frac{y}{W/2}\right)^2\right) \quad (36)$$

and

$$\langle c_{md} \rangle(x) = \bar{c}_d(0) - \frac{1}{12} \frac{Wi}{\epsilon D_e \left(1 + \xi \frac{\bar{u}_d W}{D_e}\right)} - \frac{i}{FW \bar{u}_d} x \quad (37)$$

It is interesting to note the similarity between Eqs. (17) and (37). Eq. (37) for the case of spacers may be reduced by replacing the factor $17/140$ and the diffusion coefficient D_e in Eq. (17), by $1/12$ and $\epsilon D_e (1 + \xi \bar{u}_d W / D_e)$, respectively. Hence, the limiting current density in which $\langle c_{md} \rangle(L) = 0$ is given for the case of long channel case, by

$$i_{lim} = \frac{\frac{FW \bar{u}_d}{L} \bar{c}_d(0)}{1 + \frac{1}{12} \left(\frac{\bar{u}_d W^2}{\epsilon D_e \left(1 + \xi \frac{\bar{u}_d W}{D_e}\right) L} \right)} \approx \frac{FW \bar{u}_d}{L} \bar{c}_d(0) \times \left(1 - \frac{1}{12} \left(\frac{\bar{u}_d W^2}{\epsilon D_e \left(1 + \xi \frac{\bar{u}_d W}{D_e}\right) L} \right) \right) \text{ for } \frac{\bar{u}_d W^2}{\epsilon D_e \left(1 + \xi \frac{\bar{u}_d W}{D_e}\right) L} \ll 1 \quad (38)$$

4.2. Asymptotic solutions for short channels

For the short channel regime, on the other hand, we note

$$\delta(x) \sim (\epsilon D_e (1 + \xi \frac{\bar{u}_d W}{D_e}) x / \bar{u}_d)^{1/2} \propto x^{1/2}.$$

Moreover, Eq. (10) reveals

$$(\bar{c}_d(0) - \langle c_{md} \rangle(x)) \sim (i / F \epsilon D_e (1 + \xi \frac{\bar{u}_d W}{D_e})) \delta(x) \propto x^{1/2}.$$

Thus, we define the dimensionless concentration function as

$$g(\eta) = \frac{\langle c_d \rangle(x, n) - \bar{c}_d(0)}{\langle c_{md} \rangle(x) - \bar{c}_d(0)} \quad (39)$$

with the similarity variable given by

$$\eta = \frac{n}{x} \left(\frac{\bar{u}_d x}{\epsilon D_e \left(1 + \xi \frac{\bar{u}_d W}{D_e}\right)} \right)^{1/2} \propto \frac{n}{x^{1/2}} \quad (40)$$

Using these similarity variables, Eq. (34) can readily be transformed into an ordinary differential equation as follows:

$$\frac{d^2 g}{d\eta^2} + \frac{1}{2} \left(\eta \frac{dg}{d\eta} - g \right) = 0 \quad (41)$$

which, when integrated with the boundary conditions, namely, $g(0) = 1$ and $g(\infty) = 0$, yields

$$\left. \frac{dg}{d\eta} \right|_{\eta=0} = -0.886 \quad (42)$$

From Eq. (10), we obtain

$$\begin{aligned} 2\epsilon D_e \left(1 + \xi \frac{\bar{u}_d W}{D_e} \right) \left. \frac{\partial \langle c_d \rangle}{\partial y} \right|_{y=W/2} &= -2\epsilon D_e \left(1 + \xi \frac{\bar{u}_d W}{D_e} \right) \frac{\langle c_{md} \rangle(x) - \bar{c}_d(0)}{x} \left(\frac{\bar{u}_d x}{\epsilon D_e \left(1 + \xi \frac{\bar{u}_d W}{D_e} \right)} \right)^{1/2} \left. \frac{dg}{d\eta} \right|_{\eta=0} \\ &= -\frac{i}{F} \end{aligned} \quad (43)$$

Hence, we find the limiting current density for the case of short channel:

$$i_{lim} = 1.772 F \bar{c}_d(0) \left(\frac{\bar{u}_d}{L} \epsilon D_e \left(1 + \xi \frac{\bar{u}_d W}{D_e} \right) \right)^{1/2} \text{ for } \frac{\bar{u}_d W^2}{\epsilon D_e \left(1 + \xi \frac{\bar{u}_d W}{D_e} \right) L} \gg 1 \quad (44)$$

5. Determination of stack voltage

The stack voltage (cell voltage), which refers to as the potential drop per unit cell consisting of a pair of cells and a pair of membranes, can be estimated, using Eq. (6) for the case of the sodium chloride (i.e. $z_1 = 1$ and $z_2 = -1$). Thus, the dimensionless voltage drop across the dilute cell is given by

$$\frac{F \Delta \varphi_d}{RT} = \frac{2}{D_1 + D_2} \int_0^{W/2} \left(\frac{i}{F c_d(x, n)} + (D_2 - D_1) \frac{\partial}{\partial n} \ln c_d(x, n) \right) dn \quad (45)$$

The concentration profile $c_d(x, n)$ for the case of short channel without spacers may be described approximately as

$$c_d(x, n) = \begin{cases} c_{md}(x) + \frac{i}{2FD_e} n & : 0 \leq n \leq \frac{\bar{c}_d(0) - c_{md}(x)}{(i/2FD_e)} \\ \bar{c}_d(0) & : \frac{\bar{c}_d(0) - c_{md}(x)}{(i/2FD_e)} \leq n \leq \frac{W}{2} \end{cases} \quad (46)$$

such that the profile satisfies the boundary condition at the membrane (Eq. (10)), namely,

$$D_e \left. \frac{\partial c_d}{\partial n} \right|_{n=0} = \frac{i}{2F}$$

Eq. (45) with the foregoing profile Eq. (46) can easily be integrated to find the voltage drop across the dilute cell:

$$\begin{aligned} \frac{F \Delta \varphi_d}{RT} &= \frac{Wi}{(D_1 + D_2) F \bar{c}_d(0)} \left(1 - \frac{4FD_e}{Wi} (\bar{c}_d(0) - c_{md}(x)) \right) \\ &\quad + \frac{2(2D_e + D_2 - D_1)}{D_1 + D_2} \ln \frac{\bar{c}_d(0)}{c_{md}(x)} \end{aligned} \quad (47a)$$

Likewise, we find the voltage drop across the condensate cell:

$$\frac{F\Delta\varphi_c}{RT} = \frac{\zeta Wi}{(D_1 + D_2)F\bar{c}_c(0)} \left(1 - \frac{4FD_e}{\zeta Wi} (c_{mc}(x) - \bar{c}_c(0)) \right) + \frac{2(2D_e + D_2 - D_1)}{D_1 + D_2} \ln \frac{c_{mc}(x)}{\bar{c}_c(0)} \quad (47b)$$

We assume identical feed velocities, feed concentrations and channel widths, namely, $\bar{u}_d = \bar{u}_c$, $\bar{c}_d(0) = \bar{c}_c(0)$ and $\zeta = 1$. Then, for negligible voltage drops across the cation and anion membranes, we obtain the stack voltage for channels without spacers from Eqs. (47a), (47b) and (29):

$$\begin{aligned} \frac{F(\Delta\varphi_d + \Delta\varphi_c)}{RT} &= \frac{2Wi}{(D_1 + D_2)F\bar{c}_d(0)} \left(1 - \frac{4FD_e}{Wi} (\bar{c}_d(0) - c_{md}(x)) \right) \\ &+ \frac{2(2D_e + D_2 - D_1)}{D_1 + D_2} \ln \frac{\bar{c}_d(0) + (\bar{c}_d(0) - c_{md}(x))}{\bar{c}_d(0) - (\bar{c}_d(0) - c_{md}(x))} \\ &= \frac{2Wi}{(D_1 + D_2)F\bar{c}_d(0)} \left(1 - \frac{4}{2.366} \left(\frac{D_e x}{\bar{u}_d W^2} \right)^{1/3} \right) \\ &+ \frac{2(2D_e + D_2 - D_1)}{D_1 + D_2} \ln \frac{1 + \frac{Wi}{2.366FD_e\bar{c}_d(0)} \left(\frac{D_e x}{\bar{u}_d W^2} \right)^{1/3}}{1 - \frac{Wi}{2.366FD_e\bar{c}_d(0)} \left(\frac{D_e x}{\bar{u}_d W^2} \right)^{1/3}} \end{aligned} \quad (48)$$

Likewise, from Eqs. (47a), (47b) and (43), we obtain the cell voltage for channels with spacers:

$$\begin{aligned} \frac{F(\Delta\varphi_d + \Delta\varphi_c)}{RT} &= \frac{2Wi}{(D_1 + D_2)F\bar{c}_d(0)} \left(1 - \frac{4F\varepsilon D_e \left(1 + \xi \frac{\bar{u}_d W}{D_e} \right)}{Wi} (\bar{c}_d(0) - \langle c_{md} \rangle(x)) \right) \\ &+ \frac{2 \left(2\varepsilon D_e \left(1 + \xi \frac{\bar{u}_d W}{D_e} \right) + D_2 - D_1 \right)}{D_1 + D_2} \ln \frac{\bar{c}_d(0) + (\bar{c}_d(0) - \langle c_{md} \rangle(x))}{\bar{c}_d(0) - (\bar{c}_d(0) - \langle c_{md} \rangle(x))} \\ &= \frac{2Wi}{(D_1 + D_2)F\bar{c}_d(0)} \left(1 - \frac{4}{1.772} \left(\frac{\varepsilon D_e \left(1 + \xi \frac{\bar{u}_d W}{D_e} \right) x}{\bar{u}_d W^2} \right)^{1/2} \right) \\ &+ \frac{2 \left(2\varepsilon D_e \left(1 + \xi \frac{\bar{u}_d W}{D_e} \right) + D_2 - D_1 \right)}{D_1 + D_2} \ln \frac{1 + \frac{i}{1.772F\bar{c}_d(0)} \left(\frac{x}{\bar{u}_d \varepsilon D_e \left(1 + \xi \frac{\bar{u}_d W}{D_e} \right)} \right)^{1/2}}{1 - \frac{i}{1.772F\bar{c}_d(0)} \left(\frac{x}{\bar{u}_d \varepsilon D_e \left(1 + \xi \frac{\bar{u}_d W}{D_e} \right)} \right)^{1/2}} \end{aligned} \quad (49)$$

6. Results and discussion

Fujimoto [24] carried out a careful experiment using an electrodialyser with and without spacers. The specifications in his experiment are listed in Table 1. He measured the voltage against the applied electric current and observed a marked increase in the voltage when the limiting current density was achieved as the result of incipience of water dissociation.

Table 1
Parameters in the experiment conducted by Fujimoto [24].

$\bar{c}_d(0)$	342 mol/m ³ (2%)	W	5×10^{-3} m
D_1	1.3×10^{-9} m ² /s	\bar{u}_d	0.01 ~ 0.05 m/s
D_2	2.0×10^{-9} m ² /s	T	298 K
D_e	1.575×10^{-9} m ² /s	ε	0.91
i	100 ~ 700 A/m ²	R_{cation}	$3.0 \times 10^{-4} \Omega m^2$
L	0.6 m	R_{anion}	$2.4 \times 10^{-4} \Omega m^2$

The measured values of the limiting current density for the case of electrodialyser without spacers are plotted against the feed velocity \bar{u}_d in Fig. 3(a), where the asymptotic solution for the case of short channel without spacers, namely, Eq. (30), is also presented. The cases treated in his experiment correspond to $\bar{u}_d W^2 / D_e L = 260 \sim 1300 \gg 1$, so that the short channel solution may well suffice to describe the cases. Tado [25] carried out numerical calculations solving the set of the governing equations, namely, the continuity equation, Navier-Stokes equation and Nernst-Planck equation with appropriate boundary conditions. His results, which agree well with the present asymptotic solution, are presented in the same figure. The figure indicates that both present asymptotic solution and numerical solution overestimate the limiting current density to some extent. Nevertheless, the agreement between the present analysis and measurement appears to be fairly good over a wide range of the feed velocity.

Another set of experimental data on electrodialysers without spacers were provided by Lee et al. [11], in which $\bar{u}_d W^2 / D_e L = 7700 \sim 23000 \gg 1$. The experimental details of their electrodialyser are listed in Table 2. In Fig. 3(b), their experimental data obtained for different feed concentrations are presented along with the short channel formula for the dialyser without spacers, Eq. (30), so as to see the effect of the feed concentration $\bar{c}_d(0) = \bar{c}_c(0)$ on the limiting current density. The curves based on the present analysis agree well with the experimental data for the cases of $\bar{c}_d(0) = 8$ to 50 mol/m³, whereas the analysis underestimates the limiting current density for the case of $\bar{c}_d(0) = 100$ mol/m³.

The limiting current density is solely determined from the boundary layer characteristics in the dilute channel. The comparison also reveals that the limiting current density is sensitive to the feed concentration but rather insensitive to the feed velocity, since $i_{lim} \propto \bar{u}_d^{1/3} \bar{c}_d(0)$ for the case of dialyser without spacers.

Fujimoto [24] also set up an electrodialyser with channels filled with ceramic foam with the porosity $\varepsilon = 0.91$ and conducted an experiment to investigate the effect of mechanical dispersion on the limiting current density. In Fig. 4, his experimental data on the electrodialyser with ceramic foam, which correspond to the case of short channel (i.e. $\bar{u}_d W^2 / \varepsilon D_e (1 + \xi \frac{\bar{u}_d W}{D_e}) L = 300 \sim 700 \gg 1$), are presented with the theoretical curve based on the short channel solution for the case of dialyser with porous media, namely, Eq. (44). The empirical coefficient ξ for the mechanical dispersion has been set to $\xi = 1.5 \times 10^{-5}$.

A good agreement between the present formula and the experiment can be seen from Fig. 4, which substantiates the validity of the present analysis based on the volume averaging theory. It is interesting to note that the limiting current density is almost proportional to the feed velocity, since Eq. (44) for the case of dialyser with porous media suggests $i_{lim} \propto \bar{u}_d$ for substantial mechanical dispersion. Thus, for the case of dialyser with porous media, the depletion of the ions on the membrane is retarded effectively by increasing the feed velocity \bar{u}_d .

Practical electrodialysers with spacers are designed such that the concentration boundary layer thickness is kept sufficiently thin even at the exit of the channel. Thus, most data under practical operational conditions should fall within the short channel regime. The comparison of the present formulas for the cases of with and without spacers clearly indicates that the short channel formulas (30) and (44) describe most practical cases fairly well. Hence, they can be used to estimate the limiting current density when designing electrodialysers with and without spacers. However, there will be certain cases in which the brackish water flows at very low velocity in narrow and long channels such that $\bar{u}_d W^2 / \varepsilon D_e L \ll 1$, and then, the asymptotic solution for long channel may be used to estimate the limiting current density.

Finally, in Fig. 5, the stack voltage data for the case of electrodialyser without spacers at $\bar{u}_d = \bar{u}_c = 0.05$ m/s and $\bar{c}_d(0) = \bar{c}_c(0) = 342$ mol/m³, provided by Fujimoto [24], are presented against the applied current density. In the figure, the theoretical curve based

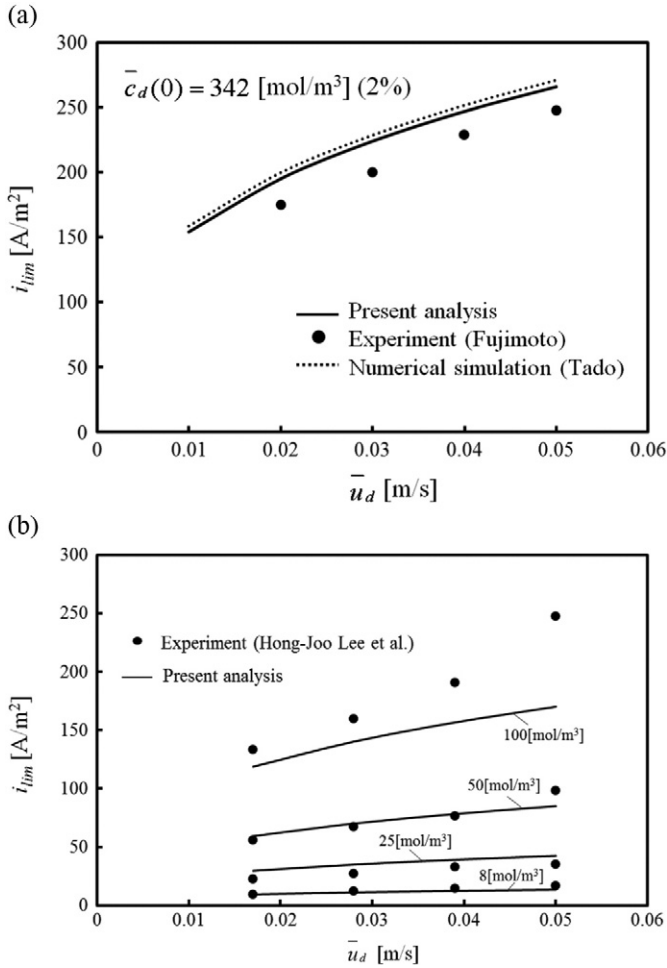


Fig. 3. Effect of feed velocity on limiting current density for the case of dialyser without spacers (a) Experimental data provided by Fujimoto [24] (b) Experimental data provided by Lee et al. [11].

on Eq. (48) is also presented for comparison. The stack voltage is the summation of the potential drops resulting from the dilute channel $\Delta\varphi_d(L)$ and the concentrate channel $\Delta\varphi_c(L)$, in addition to those resulting from the cation and anion exchange membranes, namely, $\Delta\varphi_{cell} = \Delta\varphi_d + \Delta\varphi_c + iR_{cation} + iR_{anion}$. The membrane resistances are provided by the manufacture as $R_{cation} = 3.0 \times 10^{-4} \Omega m^2$ and $R_{anion} = 2.4 \times 10^{-4} \Omega m^2$. The prediction based on Eq. (48) agrees fairly well with the experimental data towards the limiting current density, which is singular in Eq. (48). Thereafter, the stack voltage drastically increases due to the depletion of ions.

Unfortunately, the present theory based on the local electro-neutrality assumption cannot describe the ion transport mechanism beyond this depletion of ions. If a current density larger than its limiting value is applied, the drastic increase in the voltage will be followed by strong fluctuations around an average value. Krol et al. [26] pointed out that hydrodynamic instabilities close to the membrane are responsible for

Table 2

Parameters in the experiment conducted by Lee et al. [11].

$\bar{c}_d(0)$	8 ~ 100 mol/m ³	L	5.0×10^{-2} m
D_1	1.3×10^{-9} m ² /s	W	6.0×10^{-3} m
D_2	2.0×10^{-9} m ² /s	\bar{u}_d	0.017 ~ 0.05 m/s
D_e	1.575×10^{-9} m ² /s	T	298 K
i	10 ~ 250 A/m ²		

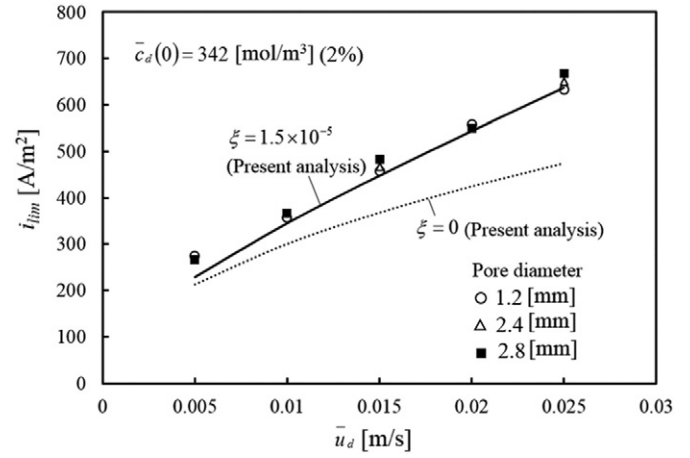


Fig. 4. Effect of feed velocity on limiting current density for the case of dialyser with porous spacers.

such fluctuations. The mechanism of the ion transport above the limiting current density is studied by Nikonenko et al. [27,28] applying the Nernst-Planck equation to both fluid and membrane phases. As pointed out by Tedesco et al. [29], non-ideal behavior of membranes such as effect of co-ion transport through the membranes is also important and should be investigated further.

7. Conclusions

A general ion transport equation valid for ion solutions has been derived from the Nernst-Planck equation by eliminating the electrophoresis term. The resulting transport equation turns out to be the conventional convection-diffusion transport equation with an effective (harmonic) diffusion coefficient. A classical boundary layer treatment was introduced to attack the ion transport equation to obtain the asymptotic similarity solutions for the short and long channel regions in electrodialysers without spacers, when the electric current is applied uniformly across the channels.

Furthermore, a volume averaging theory was exploited to transform the ion transport equation to its volume averaged version, so as to describe the transport phenomena associated with electrodialysers with spacers. Both short and long channel asymptotic solutions were obtained for the case of uniformly applied electric current, to reveal the effects of the mechanical dispersion on the limiting current density. The predicted values of the limiting current density and stack voltage based on the short channel solutions were found to agree well with the experimental data obtained using electrodialysers with and without spacers.

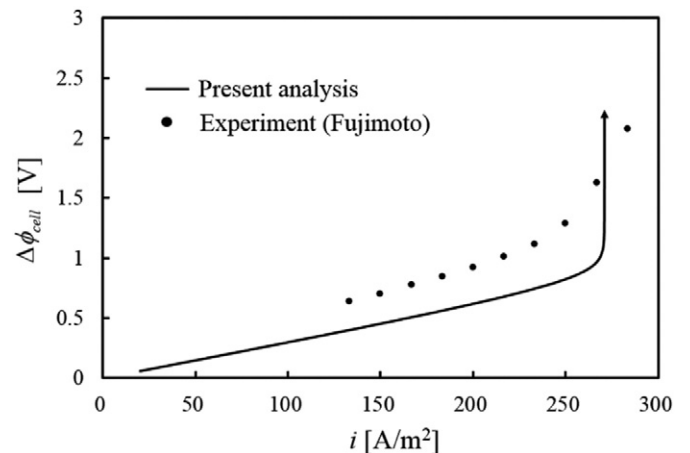


Fig. 5. Measurement of stack voltage and its comparison with the prediction.

It is clearly shown that the presence of spacers works to delay possible depletion of the ions on the dilute side of the membrane, thus increasing the limiting current density.

Acknowledgements

This work has been generously supported by the New Energy and Industrial Technology Development Organization of Japan (NEDO), under the project P13009: Research and development of geothermal energy power generation, Research and development of electrolysis scale remover for geothermal power plant. The work has been partially supported by JSPS Grants-in-Aid for Scientific Researches, Grant Number 26740049 and Grant Number 26289046. Useful technical advices provided by Prof. R. Matsushima are gratefully acknowledged.

References

- [1] H. Strathmann, Ion-Exchange Membrane Separation Processes, Elsevier, Amsterdam, 2004 1–20.
- [2] A.D. Ryabtseva, N.P. Kotsupalova, V.I. Titarenko, I.K. Igumenov, N.V. Gelfond, N.E. Fedotov, N.B. Morozov, V.A. Shipachev, A.S. Tibilov, Development of a two-stage electrodialysis set-up for economical desalination of sea-type artesian and surface waters, *Desalination* 137 (1–3) (2001) 207–214.
- [3] T. Kawahara, Construction and operation experience of a large-scale electrodialysis water desalination plant, *Desalination* 96 (1–3) (1994) 341–348.
- [4] K. Walha, R.B. Amar, L. Firdaous, F. Quemeneur, P. Jaouen, Brackish groundwater treatment by nanofiltration, reverse osmosis and electrodialysis in Tunisia: performance and cost comparison, *Desalination* 207 (1) (2007) 95–106.
- [5] A. Nakayama, Y. Sano, An application of the Sano–Nakayama membrane transport model in hollow fiber reverse osmosis desalination systems, *Desalination* 311 (2013) 95–102.
- [6] V.I. Zabolotskaya, J.A. Manzanarez, V.V. Nikonenko, K.A. Lebedev, E.G. Lovtsova, Space charge effect on competitive ion transport through ion-exchange membranes, *Desalination* 147 (2002) 1–3.
- [7] P. Sistat, G. Pourcelly, Steady-state ion transport through homopolar ion-exchange membranes: an analytical solution of the Nernst–Planck equations for a 1:1 electrolyte under the electro-neutrality assumption, *J. Electroanal. Chem.* 460 (1999) 53–62.
- [8] T. Chaabane, S. Tahab, M. Taleb Ahmed, R. Maachib, G. Dorange, Coupled model of film theory and the Nernst–Planck equation in nanofiltration, *Desalination* 206 (2007) 424–432.
- [9] A. Doyen, C. Roblet, A. L'Acheveque-Gaudet, L. Bazinet, Mathematical sigmoid-model approach for the determination of limiting and over-limiting current density values, *J. Membr. Sci.* 452 (2014) 453–459.
- [10] K. Tado, F. Sakai, Y. Sano, A. Nakayama, An analysis on ion transport process in electrodialysis desalination, *Desalination* 378 (2016) 60–66.
- [11] H.-J. Lee, H. Strathmann, S.-H. Moon, Determination of the limiting current density in electrodialysis desalination as an empirical function of linear velocity, *Desalination* 190 (2006) 43–50.
- [12] Y. Tanaka, Computer simulation of feed and bleed ion exchange membrane electrodialysis for desalination of saline water, *Desalination* 254 (2010) 517–531.
- [13] Y. Tanaka, Mass transport and energy consumption in ion-exchange membrane electrodialysis of seawater, *J. Membr. Sci.* 215 (2003) 265–279.
- [14] Y. Tanaka, Concentration polarization in ion-exchange membrane electrodialysis – the events arising in an unforced flowing solution in a desalting cell, *J. Membr. Sci.* 244 (2004) 1–16.
- [15] C.W. Tobias, M. Eisenberg, C.R. Wilke, Diffusion and convection in electrodialysis – a theoretical review, *J. Electrochem. Soc.* 99 (1952) 359–365.
- [16] A.A. Sonin, R. F. Probst, A hydrodynamic theory of desalination by electrodialysis, *Desalination* 5 (1968) 293–329.
- [17] H. Schlichting, *Boundary Layer Theory*, seventh ed. McGraw-Hill, New York, 1979.
- [18] Y. Kim, W.S. Walker, D.F. Lawler, Electrodialysis with spacers: effects of variation and correlation of boundary layer thickness, *Desalination* 274 (2011) 54–63.
- [19] A. Nakayama, *PC-Aided Numerical Heat Transfer and Convective Flow*, CRC Press, Boca Raton, 1995 17–21.
- [20] P. Cheng, Heat transfer in geothermal systems, *Adv. Heat Tran.* 14 (1978) 1–105.
- [21] M. Quintard, S. Whitaker, Local thermal equilibrium for transient heat conduction: theory and comparison with numerical experiments, *Int. J. Heat Mass Transfer* 38 (1995) 2779–2796.
- [22] M. Quintard, S. Whitaker, One and two equation models for transient diffusion processes in two-phase systems, *Adv. Heat Tran.* 23 (1993) 369–465.
- [23] W. Zhang, W. Li, A. Nakayama, An analytical consideration of steady state forced convection within a nanofluid saturated metal foam, *J. Fluid Mech.* 769 (2015) 590–620.
- [24] R. Fujimoto, A Study on Efficiency Enhancement of Seawater Desalination by Electrodialysis, M.S. Thesis, Okayama University, March 2016.
- [25] K. Tado, A Mathematical Model for Desalination-Concentration Process by Electrodialysis, M.S. Thesis, Shizuoka University, March 2015.
- [26] J.J. Krol, M. Wessling, H. Strathmann, Chronopotentiometry and overlimiting ion transport through monopolar ion exchange membranes, *J. Membr. Sci.* 162 (1999) 155–164.
- [27] V.V. Nikonenko, N.D. Pismenskaya, E.I. Belova, P. Sistat, P. Hugué, G. Pourcelly, C. Larchet, Intensive current transfer in membrane systems: modelling, mechanisms and application in electrodialysis, *Adv. Colloid Interface Sci.* 160 (2010) 101–123.
- [28] V.V. Nikonenko, A.V. Kovalenko, M.K. Urtenov, N.D. Pismenskaya, J. Han, P. Sistat, G. Pourcelly, Desalination at overlimiting currents: state-of-the-art and perspectives, *Desalination* 342 (2014) 85–106.
- [29] M. Tedesco, H.V.M. Hamelers, P.M. Biesheuvel, Nernst–Planck transport theory for (reverse) electrodialysis: I. Effect of co-ion transport through the membranes, *J. Membr. Sci.* 510 (2016) 370–381.